Fabrication of metal nanodots and nanowires by atomic force microscopy nanomachining

Heh-Nan Lin (Electronic mail: hnlin@mx.nthu.edu.tw)

Department of Materials Science and Engineering,
National Tsing Hua University, Hsinchu 30013, Taiwan

Abstract

The fabrication of metal nanostructures by a combination of atomic force microscopy nanomachining on a thin polymer resist, metal coating and lift-off is reported. Nanodots with sizes and nanowires with widths ranging between 50 and 100 nm have been successfully created. The present work exemplifies the feasibility and effectiveness of using a single-layer resist in comparison with a two-layer resist. In addition, the localized surface plasmon resonance peaks of the metal nanostructures have been measured and the selective growths of zinc oxide nanowires on the metal nanostructures are demonstrated.

1. Introduction

Metal nanostructures have been the focus of extensive research activities in recent years due to their unusual electrical, magnetic and optical properties, and applications as masks for chemical etching, templates for immobilization of bio-receptors,[1] chemical sensors,[1,2] catalysts for the selective growth of nanomaterials,[3] nano-photonic devices,[4] nanointerconnects,[5] data storage bits,[6] etc. Fabrication techniques are naturally of great interest, and various physical, chemical or even biological approaches have been developed. In particular, scanning probe lithography (SPL)[7] has been employed since more than a decade ago and in continual usage and improvement due to the advantages of ease of operation and relatively low cost. Among the various SPL techniques, atomic force microscopy (AFM) nanomachining has been adopted since the early years.[8] By controlling the contact force between the AFM tip and the sample, desired nanopatterns can be created. Furthermore, with the use of a resist and the application of a subsequent lift-off process, metal nanodots (NDs) and nanowires (NWs) with widths down to 40 nm have been fabricated.[9–11] However, the resists in reported works usually have a bi-layer or tri-layer structure[9–11] and are more complicated than a single-layer resist. This study reports the successful fabrication of metal NDs and NWs with the use of a single-layer resist.[12,13] Furthermore, the surface plasmon resonance peaks of the metal nanostructures have been measured and the selective growths of zinc oxide NWs on the metal nanostructures are demonstrated.[14]

2. Experiment

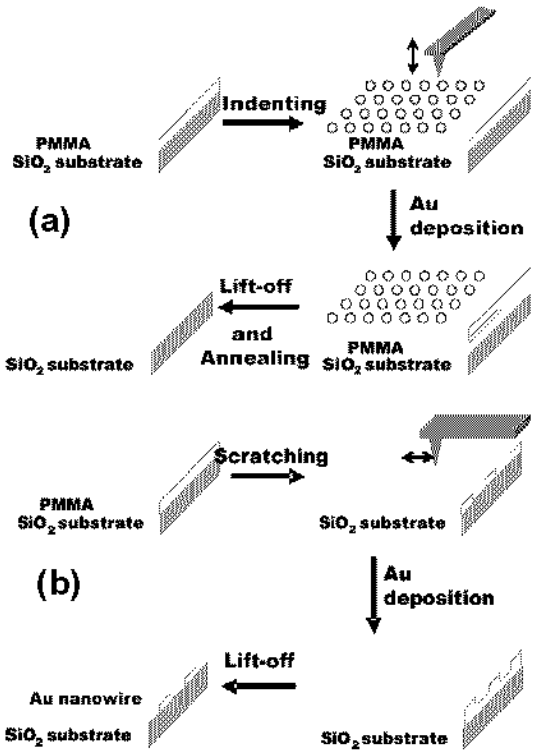

Fig.1 Schematic diagram of the experimental procedures for the fabrication of metal (a) NDs and (b) NWs, respectively

The resist was made of a 50 nm thick PMMA film and prepared by spin-coating on a Si or a sapphire substrate. A commercial AFM (Smena-B, NT-MDT, Russia) and rectangular silicon probes (NSC15, MikroMasch, Russia) were employed for the experiment. The AFM was operated in the intermittent-contact mode for imaging. The experimental procedures are depicted in Figs. 1(a) and 1(b) for NDs and NWs, respectively. Each indentation was realized by moving the tip in the vertical direction toward the sample. A desired pattern of holes was created by locating the tip on designated positions controlled by the software. A straight groove could also be produced by indenting and moving the tip along a straight line. A metal film was then coated on the sample by e-beam evaporation or sputtering. The sample was soaked in acetone in an ultrasonic bath to remove the resist and finally dried by nitrogen gas. Details of the experimental procedures can be found in our previous publications.[12,13]

3. Results and discussion

With the use of an indentation force of 3.8 μN, a nanohole array was generated on the PMMA film on a sapphire substrate and the AFM image is shown in Fig. 2(a). The pile-up around each hole is apparent, which is similar to those reported previously. After coating a 10 nm thick gold film and removing the PMMA, a gold ND array with a smallest dot size of around 70 nm was fabricated and the result is shown in Fig. 2(b).[12] In addition to regular arrays, complicated dot patterns were also constructed. In Fig. 2(c), the scanning electron microscope (SEM) image of a pattern "NANO" is presented. With the use of different forces, NDs with sizes down to 20 nm can be created and the results are shown in Fig. 2(d). The AFM images of a nanogroove array after nanoscratching and a single nanogroove are shown in Figs. 3(a) and 3(b), respectively. The nanogrooves appear as though they are elevated lines in Fig. 3(a) due to the pile-up of the displaced polymer, which was also observed in previous works. The SEM image of the gold NWs fabricated from the pattern is shown in Fig. 3(c). A zoomed image is presented in Fig. 3(d) and the width is around 70 nm. By similar scratching, contact pads were connected to a single NW and a linear current-voltage relationship was observed. Various NWs of different metals have been fabricated and the results are summarized in Table 1.[13]

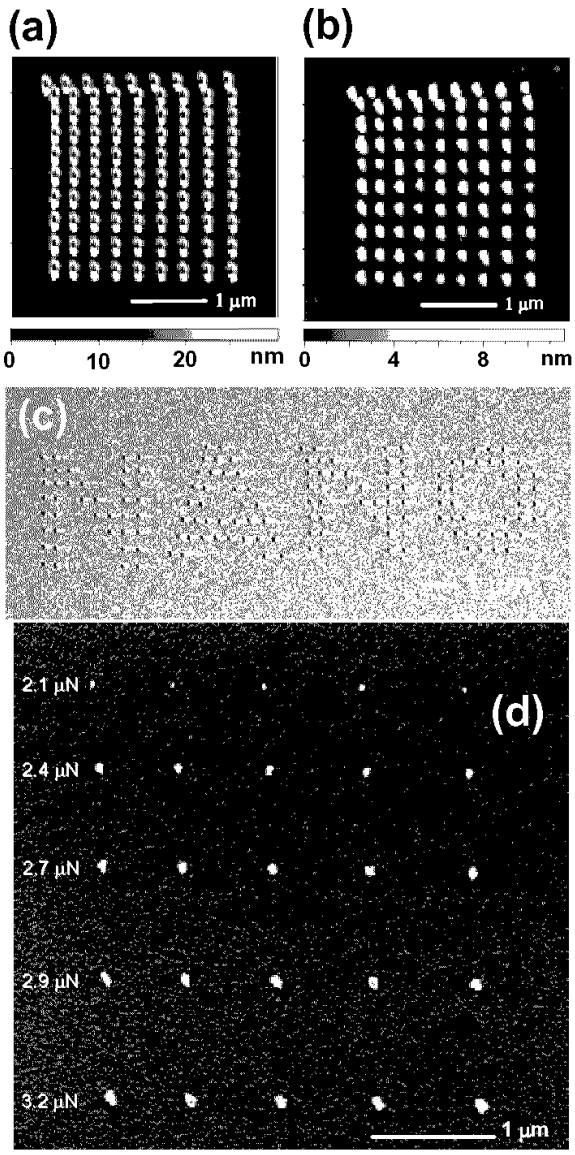

Fig. 2 AFM images of (a) a nanohole array on PMMA and (b) the corresponding gold nanodot array after lift-off. SEM images of (c) a gold ND pattern "NANO" on sapphire and (d) gold NDs on silicon created with different forces.

The localized surface plasmon resonance (LSPR), which is the collective oscillation of conduction electrons in metal with incident optical wave at a specific frequency,[1] of the NDs and the NWs were studied by using dark-field optical microscopy. The SEM image of a gold ND array after thermal annealing at 900 °C is shown in Fig. 4(a). From a zoomed image shown in Fig. 4(b), the average diameter is around 72 nm. The optical image of the array is presented in Fig. 4(c) and appears green. The scattering spectrum is plotted in Fig. 4(d) and the resonance peak is located at 548 nm, which is consistent with reports in the literature.

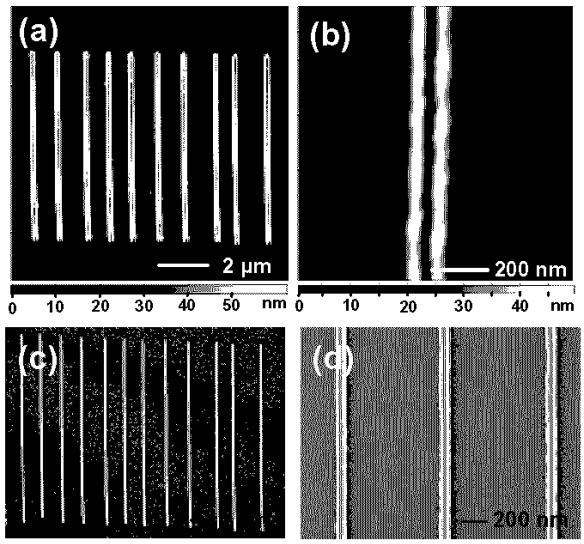

Fig. 3 AFM images of (a) a nanogroove array after nanoscratching and (b) a single nanogroove. SEM image of (c) the gold NWs fabricated from the pattern and (d) a single NW showing the width is around 70 nm.

Table 1 Widths, lengths, thicknesses, resistances and resistivities of various NWs and comparative resistivities reported in literature.

	W(nm)	*L*(μm)	*T*(nm)	*R*(Ω)	$\rho(\mu\Omega\cdot cm)$	$\rho(\mu\Omega\cdot cm)$ *in literature*	Bulk $\rho(\mu\Omega\cdot cm)$
Au	60	3.9	15	595	13.7	7	2.35
	65	10.2	15	1255	12.0	6	
	65	11.5	15	1462	12.4	30	
	70	9.8	15	987	10.6	13	
Cu	50	3.5	15	1310	28.1	17	1.67
	50	4.4	15	2227	37.0		
	50	6.5	15	2793	32.2		
	60	6.4	20	926	17.4		
Ni	50	7.0	10	7531	53.8	9 3x	6.84
	55	15.6	10	10205	36.0		
	60	3.7	10	3267	53.0		
	65	5.4	10	4486	54.0		
Al	50	8.0	10	2545	15.9	NA	2.65
Ti	50	12.0	10	358k	1492	130	42
	55	10.9	10	213k	1074		

The localized surface plasmon resonance (LSPR), which is the collective oscillation of conduction electrons in metal with incident optical wave at a specific frequency,[1] of the NDs and the NWs were studied by using dark-field optical microscopy. The SEM image of a gold ND array after thermal annealing at 900 °C is shown in Fig. 4(a). From a zoomed image shown in Fig. 4(b), the average diameter is around 72 nm. The optical image of the array is presented in Fig. 4(c) and appears green. The scattering spectrum is plotted in Fig. 4(d) and the resonance peak is located at 548 nm, which is consistent with reports in the literature. The SEM image of a gold NW array and a zoomed view of a single NW are shown in Figs. 5(a) and 5(b), respectively. The NWs have a thickness of 20 nm and a width of 50 nm. The optical image of the array is presented in Fig. 5(c) and appears bright and reddish. The scattering spectrum is plotted in Fig. 5(d) and composed of two resonance peaks in the blue and the red regions. It is also found that when the width is increased, the red peak experiences a red shift, whereas the blue peak remains unchanged. It is clear that the two peaks can be attributed to resonances along the thickness and width directions of the NWs.

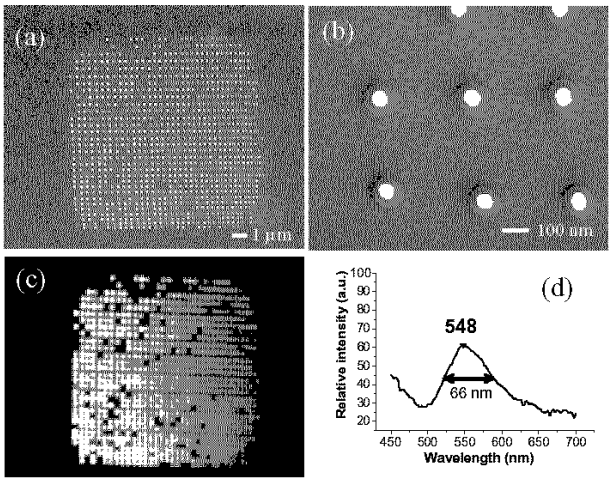

Fig. 4 SEM images of (a) a gold ND array and (b) a zoomed view of the NDs after thermal annealing at 900 °C. (c), (d) Optical image, which appears green, and spectrum of (a), respectively.

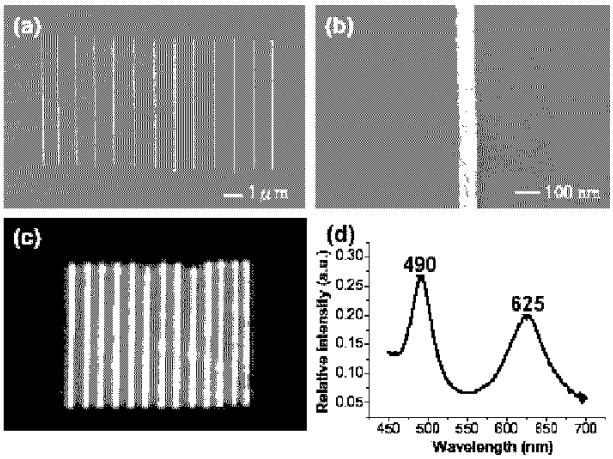

Fig. 5 SEM images of (a) a gold NW array and (b) a zoomed view of a single NW. (c), (d) Optical image, which appears bright and reddish, and spectrum of (a), respectively.

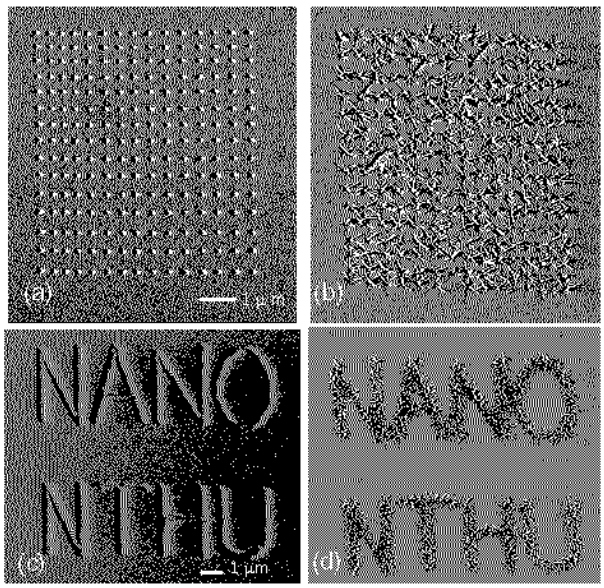

Fig. 6 SEM images of (a) a gold ND array and (c) a gold nanopatterns on sapphire substrates, and (b), (d) the corresponding zinc oxide NWs grown on (a), (c), respectively

The metal nanostructures were also used as catalysts for the selective growth of oxide NWs. The SEM images of a gold ND array and a gold nanopatterns "NANO NTHU" on sapphire substrates are shown in Figs. 6(a) and 6(c), respectively. The SEM images of the corresponding zinc oxide NWs grown on Figs. 6(a) and 6(c) by thermal evaporation are shown in Figs. 6(b) and 6(d), respectively.[14] The NWs in Fig. 6(b) have a rather uniform diameter of around 20 nm, whereas the diameters of the NWs in Fig. 6(d) are more diverse. The results indicate that the size of the NWs can be effectively controlled by the catalyst size. Similar observation has been found from the selective growth of silica NWs.[15]

4. Conclusion

A combination of AFM nanomachining and lift-off process based on the one-layer approach is a convenient method for the fabrication of metal nanostructures. The generation of metal NDs and NWs has been realized. The LSPR spectra of these nanostructures have been measured. The selective growths of zinc oxide NWs on various nanostructures have been accomplished. It is apparent that probe storage related techniques are valuable for the fabrication of metal nanostructures and subsequent applications.

Acknowledgment

Current and previous members in the author's group are gratefully acknowledged. This work was supported by the National Science Council under Grant No. 95-2221-E-007-097 and the U. S. Air Force under Grant No. AOARD-06-4074.

Reference

[1] A. J. Haes, D. A. Stuart, S. Nie, and R. P. 2004, Van Duyne, J. Fluoresc. 14, 355.
[2] M. Yun, N. V. Myung, R. P. Vasquez, C. Lee, E. Menke, and R. M. Penner, 2004, Nano Lett. 4, 419.
[3] H. J. Fan, P. Werner, and M. Zacharias, 2006, Small 2, 700.
[4] H. Ditlbacher et al., 2005, Phys. Rev. Lett., 95, 257403.
[5] G. Schindler, G. Steinlesberger, M. Engelhardt, and W. Steinhögl, 2003, Solid-State Electron. 47, 1233.
[6] M. Hehn, K. Ounadjela, J.-P. Bucher, F. Rousseaux, D. Decanini, B. Bartenlian, and C. Chappert, 1996, Science 272, 1782.
[7] H. T. Soh, K. W. Guarini, and C. F. Quate, 2001, Scanning Probe Lithography (Kluwer, Boston, 2001).
[8] Y. Kim and C. M., 1992, Lieber, Science 257, 375.
[9] L. L. Sohn and R. L., 1995, Willett, Appl. Phys. Lett. 67, 1552.
[10] V. Bouchiat and D. Esteve, 1996, Appl. Phys. Lett. 69, 3098.
[11]S. Hu, A. Hamidi, S. Altmeyer, T. Köster, B. Spangenberg, and H. Kurz, 1998, J. Vac. Sci. Technol. B 16, 2822.
[12]J.-H. Hsu, C.-Y. Lin, and H.-N. Lin, 2004, J. Vac. Sci. Technol. B 22, 2768.
[13]Y.-J. Chen, J.-H. Hsu, and H.-N. Lin, 2005, Nanotechnology 16, 1112.
[14]J. H. He, J. H. Hsu, C. W. Wang, H. N. Lin, L. J. Chen, and Z. L. Wang, 2006, J. Phys. Chem. B 110, 50.
[15]J.-H. Hsu, M.-H. Huang, H.-H. Lin, and H.-N. Lin, 2006, Nanotechnology 17, 170.